Research Square

Preprints are preliminary reports that have not undergone peer review.
They should not be considered conclusive, used to inform clinical practice,
or referenced by the media as validated information.

Disentangling the Synergistic Mechanisms of Urban Waterlogging Risks in High-Density Coastal Cities: A Quantitative Contribution Analysis

Yan Long
Hebei University of Engineering
Shumin Jiang
Hebei University of Engineering
Tongxin Yang
2793714715@qq.com

Beijing Normal University
Yikai Hou
Hebei University of Engineering
Yifan Chen
Zhejiang University of Water Resources and Electric Power
Xiaohui Lei
Hebei University of Engineering
Chenfei Duan
Hebei University of Engineering

Research Article

Keywords: Compound flooding, Urban resilience, Coupled hydrodynamic modeling, Interaction effects, Coastal cities, Disaster mitigation

Posted Date: April 8th, 2026

DOI: https://doi.org/10.21203/rs.3.rs-9021318/v1

License: This work is licensed under a Creative Commons Attribution 4.0 International License.
Read Full License

Disentangling the Synergistic Mechanisms of Urban Waterlogging Risks in High-Density Coastal Cities: A Quantitative Contribution Analysis

Yan Long[a,b] , Shumin Jiang[a,b], Tongxin Yang[c*], Yikai Hou[a,b], Yifan Chen[d], Xiaohui Lei[a,b], Chenfei Duan[a,b]

[a] *School of Water Resources and Electric Power, Hebei University of Engineering, Handan, Hebei Province, 056038, China*

[b] *Hebei Key Laboratory of Smart Water Conservancy, Hebei University of Engineering, Handan, Hebei Province, 056038, China*

[c] *School of Environment, Beijing Normal University, Beijing, 100875, China*

[d] *College of Water Conservancy and Environmental Engineering, Zhejiang University of Water Resources and Electric Power, Hangzhou 310018, China*

*Corresponding author: Tongxin Yang

E-mail address: 2793714715@qq.com

Mailing Address: 19 Taiji Road, Handan Economic and Technological Development Zone, Handan City, Hebei Province, 056038, China

Abstract

High-density coastal cities face escalating risks from compound flooding driven by drainage limitations and natural hydrometeorological extremes. However, underexplored non-linear interactions between these factors hinder effective mitigation. Focusing on Shalang District, Zhongshan City, China, this study proposes a quantitative framework to disentangle the contribution rates and interaction effects of critical factors: insufficient drainage capacity, low-lying terrain, and river backwater effects. A coupled 1D-2D model integrating the Storm Water Management Model (SWMM) and the Integrated Terrestrial Fluxes Model (ITF-FLOOD) was constructed to simulate inundation scenarios under varying rainfall return periods. An improved contribution rate calculation method based on factorial scenario analysis is adopted to quantify the synergistic and antagonistic mechanisms driving waterlogging severity. Results reveal that while insufficient drainage capacity is the dominant factor (contributing 30% - 109% to overflow volume), its influence is non-linearly modulated by natural boundary conditions. A critical antagonistic effect between drainage capacity and low-lying terrain is identified, suggesting that in deep depressions, simply upgrading pipe networks yields diminishing returns. Conversely, the river backwater effect exhibits a dynamic amplification mechanism: its contribution rate significantly escalates with the rainfall return period (surging from 16% to 65% at critical nodes), acting as a major constraint on drainage efficiency. The study concludes that single-measure retrofitting is insufficient for resilient flood management. Instead, a synergistic strategy integrating drainage network expansion with active river level regulation is essential to break the hydraulic lock in coastal urban areas. These findings provide a theoretical basis for prioritizing

retrofit investments in complex urban water systems.

Keywords: Compound flooding; Urban resilience; Coupled hydrodynamic modeling; Interaction effects; Coastal cities; Disaster mitigation

1 Introduction

In the context of global climate warming, the frequency and intensity of extreme rainfall events have risen sharply (Li et al., 2024), exacerbating the vulnerability of high-density urban areas to waterlogging disasters. Urban waterlogging has evolved into a persistent threat to sustainable urban development (Lin et al., 2022), with risks showing a continuous upward trend (Xu et al., 2024). This challenge is particularly acute in coastal and tidal river network cities, where drainage systems are often constrained by complex boundary conditions. Unlike inland cities, these areas face compound flooding driven by the superposition of heavy precipitation, high river water levels, and impervious surface expansion (Pan, 2025). Consequently, urban waterlogging management has become a pressing practical issue that requires a deep understanding of the causative mechanisms.

The formation of urban waterlogging is a complex process involving intricate interactions between environmental and anthropogenic factors (Wang et al., 2018; Komori et al., 2022). Existing studies have extensively identified key drivers, such as precipitation variability, rapid urbanization, and topography (Zhao et al., 2023; Han et al., 2024). For instance, urbanization significantly alters underlying surfaces, increasing runoff coefficients and accelerating convergence (Zheng et al., 2023). Meanwhile, the performance of drainage systems, specifically

insufficient pipe capacity and flawed network topology, has been widely recognized as a critical anthropogenic constraint (Jin et al., 2023; Ding and Xi, 2024). Recent research has also highlighted the multi-scale driving effects of urban spatial structure and population density on flood risks (Zhang et al., 2021; Wu et al., 2023).

However, a critical gap remains in the current literature: most studies treat these factors in isolation or rely on linear correlation analyses to describe their impacts (Singh et al., 2023). In reality, the factors driving waterlogging do not act independently; they exhibit strong non-linear interactions (Luan et al., 2024). For example, in tidal river network cities, the effectiveness of drainage pipe expansion is often non-linearly modulated by the river backwater effect. Standard statistical methods, such as Pearson correlation or Principal Component Analysis (Komori et al., 2022), fail to capture these synergistic or antagonistic mechanisms. Due to the lack of quantification regarding these interaction effects, it is difficult to determine the optimal retrofitting strategy, whether to prioritize pipe network expansion, pump station construction, or river dredging, under limited budget constraints (Fan and Wang, 2023).

To address these challenges, this study proposes a novel quantitative framework to disentangle the synergistic mechanisms of urban waterlogging risks. Taking the Shalang area in Zhongshan City, a typical high-density coastal area susceptible to tidal backwater effects, as the study site, a coupled 1D-2D hydrodynamic model (SWMM and ITF-FLOOD) is established to achieve high-resolution simulations (Zhai, 2023). Unlike traditional sensitivity analyses, a factorial scenario analysis method is used to quantify the contribution rates of three critical factors: insufficient drainage capacity, low-lying terrain, and the river backwater effect. This study aims

to: (1) quantify the relative importance of anthropogenic and natural factors under different rainfall return periods; (2) reveal the synergistic and antagonistic interaction mechanisms between drainage capacity and boundary conditions; and (3) provide evidence-based strategies for resilient urban flood management.

2 Study area

The study focuses on the Shalang drainage area, located in the West District of Zhongshan City, Guangdong Province, China (Fig. 1). Situated in the hinterland of the Pearl River Delta, the area covers approximately 13.66 km^2 and serves as a representative example of a high-density coastal urbanization zone. The region is governed by a subtropical monsoon climate, characterized by abundant thermal energy and substantial precipitation. The rainfall exhibits significant temporal variability, with uneven intra-annual distribution and frequent high-intensity storm events, making the region highly susceptible to hydrometeorological hazards throughout the year.

Topographically, the study area is predominantly flat and low-lying, typical of deltaic plains. It is encircled and intersected by a dense network of tidal rivers. This specific geographical configuration creates a critical hydraulic constraint: during storm surges or high tides, elevated river water levels frequently generate significant backwater effects, obstructing the gravity drainage of the urban pipe network. Furthermore, rapid urbanization has led to extensive impervious surfaces, which, combined with the low-lying terrain and aging drainage infrastructure (e.g., root intrusion defects), exacerbates the compound flooding risk driven by the

superposition of heavy rainfall and high downstream boundary conditions. Historical records (2022 - 2024) indicate severe waterlogging issues in the area. Critical areas exhibit high inundation frequency and prolonged duration, validating the urgency of this study.

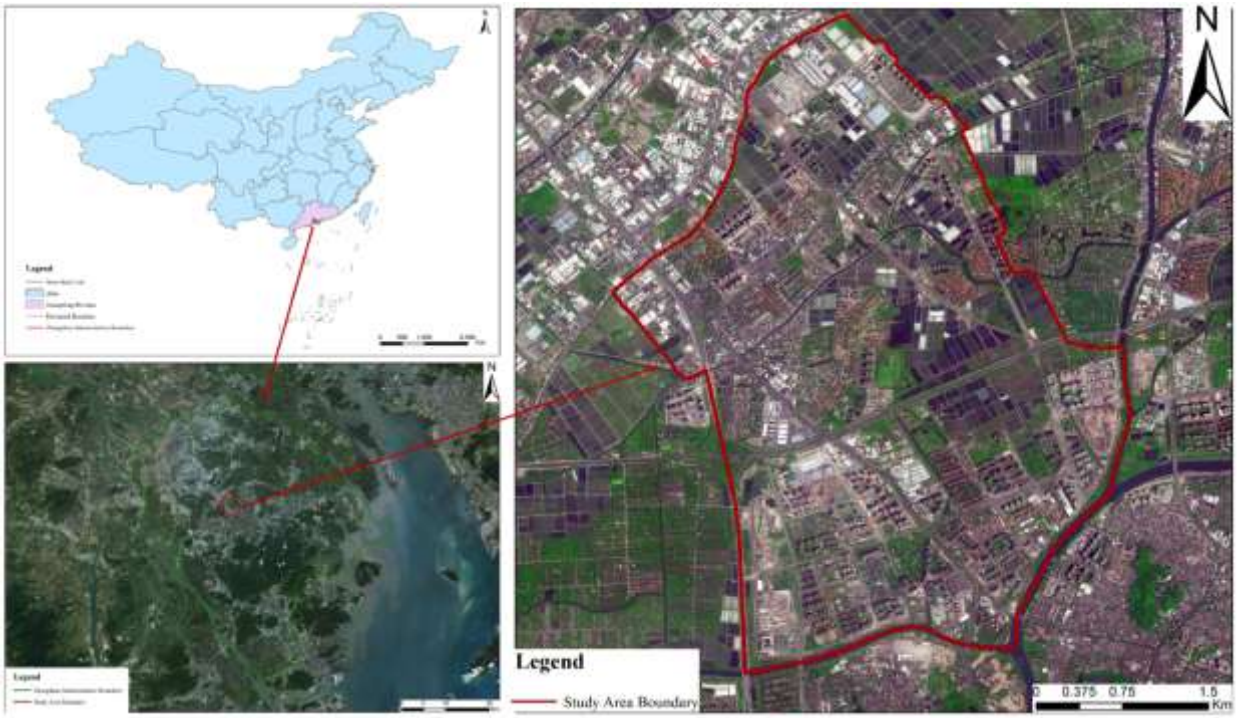


Fig. 1. Geographical location map of the study area.

3 Methodology

To quantitatively disentangle the complex interaction mechanisms driving urban waterlogging risks, this study establishes a comprehensive research framework comprising three modules: (1) a high-resolution coupled hydrodynamic model construction; (2) a factorial scenario design based on sensitivity analysis; and (3) a quantitative contribution rate method rooted in interaction theory. The workflow is illustrated in Fig. 2.

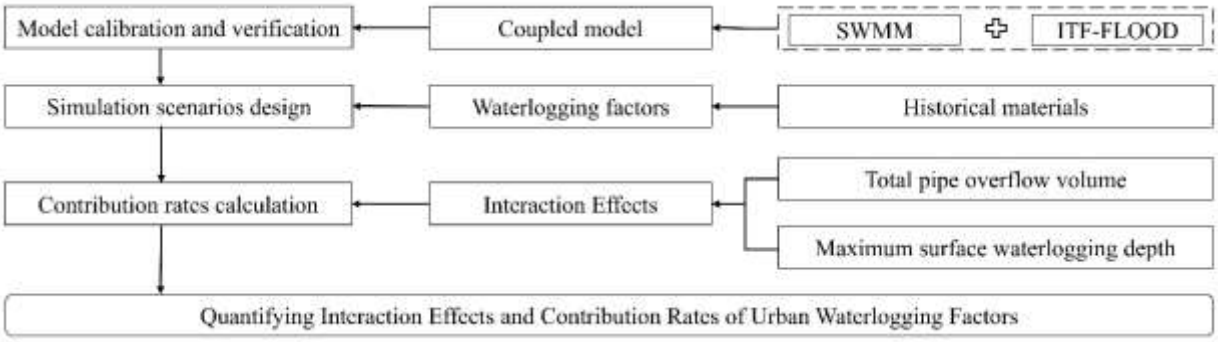


Fig. 2. Framework diagram

3.1 Coupled Hydrodynamic Modeling Framework

Given the complex interplay between underground pipe flows and surface inundation in high-density urban areas, a coupled 1D-2D modeling approach was adopted. The Storm Water Management Model (Huber et al., 2005) was employed to simulate the 1D underground drainage processes, including runoff generation and pipe flow routing. To capture the detailed spatiotemporal evolution of surface flooding, the ITF-FLOOD model, a 2D hydrodynamic model developed by the China Institute of Water Resources and Hydropower Research, was utilized. The ITF-FLOOD model leverages a two-tiered parallel architecture (MPI + OpenMP) and GPU acceleration technology, enabling high-efficiency simulation of surface water movements over high-resolution grids.

A one-way coupling strategy was implemented to integrate the two models. Specifically, the node overflow processes simulated by SWMM serve as point source inputs for the ITF-FLOOD model to drive surface inundation evolution. While fully bidirectional coupling offers higher theoretical fidelity, a one-way coupling strategy was adopted in this study to balance computational efficiency with accuracy. Field investigations indicate that during extreme rainfall

events in the study area, the dominant process is the surcharge-induced overflow from the pipe network onto the surface. Therefore, this coupling method effectively captures the primary mechanism of waterlogging formation while facilitating the rapid computation required for the extensive scenario analysis in this study.

3.2 Quantitative Framework for Disentangling Synergistic Mechanisms

Traditional statistical methods often fail to capture the non-linear synergistic or antagonistic effects among multiple flood drivers. To address this, this work proposes an improved contribution rate calculation method based on factorial analysis.

3.2.1 Factor Identification

Based on historical waterlogging data (2022 - 2024) (Fig. 3) and field surveys in the study area, three critical causative factors were identified: (1) Insufficient Drainage Capacity, manifested by pipe surcharges; (2) Low-lying Terrain, which creates local depressions; and (3) River Backwater Effect, caused by high tidal water levels obstructing gravity drainage.

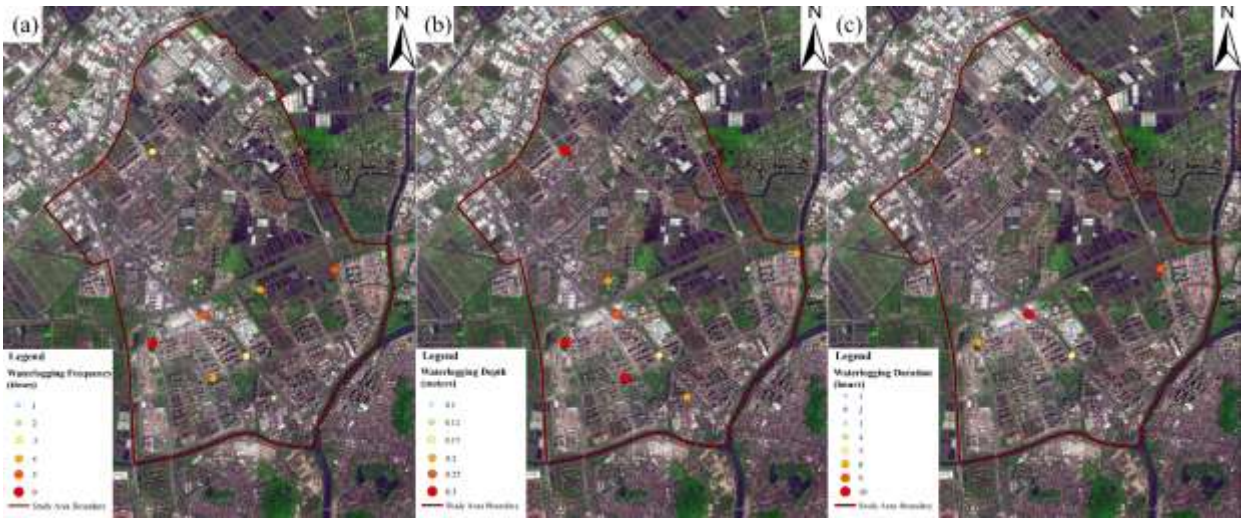


Fig. 3. Spatial distribution of waterlogging severity indicators: **(a)** waterlogging frequency, **(b)** waterlogging depth

and **(c)** waterlogging duration.

Based on the analysis results, three typical points were selected for further study: Node J1 with the most frequent waterlogging, maximum waterlogging depth and long duration; Node J2 with frequent waterlogging, large waterlogging depth and the longest duration; and Node J3 with frequent waterlogging, small waterlogging depth and long duration. The study focused on the influences of each waterlogging factor on the total overflow volume and maximum waterlogging depth at these points.

3.2.2 Calculation of Interaction Effects and Contribution Rates

The core principle of this method is to decompose the total waterlogging severity into the main effects of individual factors and their multi-order interaction effects. The contribution rate was initially applied in economic benefit evaluation. The principle is to quantify the contribution degree of various factors to economic growth using statistical methods, calculated as the ratio of the contribution amount of a particular factor to the total contribution amount, which can reflect the importance or influence of this factor in the overall context (Zou et al., 2023).

(1) Total impact:

$$\Delta^{i}_{Total} = R^{i}_{together} - R_{basis} \quad (1)$$

Where, Δ^{i}_{Total} represents the actual total impact of the simultaneous change of the three waterlogging factors under the i-th scenario; $R^{i}_{together}$ represents the simulation results of the simultaneous changes of the three waterlogging factors under the i-th scenario; R_{basis} represents the simulation results under the baseline scenario.

(2) Main effect of a single waterlogging factor:

$$M^{i}_{flow} = R^{i}_{flow} - R_{basis} \quad (2)$$

Where, M^{i}_{flow} represents the actual total impact under the i-th scenario when the insufficient drainage capacity; R^{i}_{flow} represents the simulation results for the i-th scenario when the insufficient drainage capacity.

$$M^{i}_{elevation} = R^{i}_{elevation} - R_{basis} \quad (3)$$

Where, $M^{i}_{elevation}$ represents the actual total impact in the i-th scenario when low-lying terrain; $R^{i}_{elevation}$ represents the simulation result in the i-th scenario when low-lying terrain.

$$M^{i}_{river} = R^{i}_{river} - R_{basis} \quad (4)$$

Where, M^{i}_{river} represents the actual total impact during the river backwater effect in the i-th scenario; R^{i}_{river} represents the simulation result during the river backwater effect in the i-th scenario.

(3) Second-order interaction effect of two waterlogging factors:

$$T^{i}_{fe} = R^{i}_{fe} - R_{basis} \quad (5)$$

$$A^{i}_{fe} = M^{i}_{flow} + M^{i}_{elevation} \quad (6)$$

$$I^{i}_{fe} = T^{i}_{fe} - A^{i}_{fe} \quad (7)$$

Where, T^{i}_{fe} represents the actual total impact of the combined effect of drainage capacity of pipe network shortage and low-lying terrain in the i-th scenario; R^{i}_{fe} represents the simulation results of the two waterlogging factors in the i-th scenario; A^{i}_{fe} represents the theoretical total impact of the combined effect of the two waterlogging factors in the i-th scenario; I^{i}_{fe} represents the second-order interaction effect of the two waterlogging factors in the i-th scenario.

$$T^{i}_{fr} = R^{i}_{fr} - R_{basis} \quad (8)$$

$$A^{i}_{fr} = M^{i}_{flow} + M^{i}_{river} \quad (9)$$

$$I^i_{fr} = T^i_{fr} - A^i_{fr} \tag{10}$$

Where, T^i_{fr} represents the actual total impact of the combined action of insufficient drainage capacity and river backwater effect in the i-th scenario; R^i_{fr} represents the simulation result of the combined action of the two waterlogging factors in the i-th scenario; A^i_{fr} represents the theoretical total impact of the combined action of the two waterlogging factors in the i-th scenario; I^i_{fr} represents the second-order interaction effect of the two waterlogging factors in the i-th scenario.

$$T^i_{er} = R^i_{er} - R_{basis} \tag{11}$$

$$A^i_{er} = M^i_{elevation} + M^i_{river} \tag{12}$$

$$I^i_{er} = T^i_{er} - A^i_{er} \tag{13}$$

Where, T^i_{er} represents the actual total impact of the combined action of low-lying terrain and river backwater effect in the i-th scenario; R^i_{er} represents the simulation result of the combined action of the two waterlogging factors in the i-th scenario; A^i_{er} represents the theoretical total impact of the combined action of the two waterlogging factors in the i-th scenario; I^i_{er} represents the second-order interaction effect of the two waterlogging factors in the i-th scenario.

When the second-order interaction effect is greater than 0, it indicates a synergistic effect between these two waterlogging factors. When the second-order interaction effect is less than 0, it shows an antagonistic effect between the two waterlogging factors.

(4) Third-order interaction effects:

$$A^i_{together} = M^i_{flow} + M^i_{elevation} + M^i_{river} + I^i_{fe} + I^i_{fr} + I^i_{er} \tag{14}$$

$$I^i_{together} = \Delta^i_{Total} - A^i_{together} \tag{15}$$

Where, $A^i_{together}$ represents the theoretical total impact of the combined action of the three

206 waterlogging factors in the i-th scenario; $I^{i}_{together}$ represents the third order interaction effect of
207 the combined action of the three waterlogging factors in the i-th scenario.

208 When the third-order interaction effect is greater than 0, it indicates a synergistic effect
209 among these three waterlogging factors. When the third-order interaction effect is less than 0, it
210 shows an antagonistic effect among them.

211 (5) Contribution rates:

212 To translate these physical effects into actionable insights, contribution rates are calculated.
213 Drawing upon the principle of fair attribution in cooperative game theory (analogous to the
214 Shapley value), the interaction effects are equally allocated to the participating factors. For
215 example, the contribution rate of insufficient drainage capacity (C^{i}_{flow}) under the influence of three
216 factors is derived as follows:

217 $$C^{i}_{flow} = \frac{M^{i}_{flow} + \frac{I^{i}_{fe}}{2} + \frac{I^{i}_{fr}}{2} + \frac{I^{i}_{together}}{3}}{\Delta^{i}_{Total}} \times 100\% \quad (16)$$

218 $$C^{i}_{elevation} = \frac{M^{i}_{elevation} + \frac{I^{i}_{fe}}{2} + \frac{I^{i}_{er}}{2} + \frac{I^{i}_{together}}{3}}{\Delta^{i}_{Total}} \times 100\% \quad (17)$$

219 $$C^{i}_{river} = \frac{M^{i}_{river} + \frac{I^{i}_{fr}}{2} + \frac{I^{i}_{er}}{2} + \frac{I^{i}_{together}}{3}}{\Delta^{i}_{Total}} \times 100\% \quad (18)$$

220 Where, C^{i}_{flow} represents the contribution rate of the insufficient drainage capacity in the i-th
221 scenario under the combined effects of three waterlogging factors: insufficient drainage capacity,
222 low-lying terrain, and river backwater effect; $C^{i}_{elevation}$ represents the contribution rate of low-
223 lying terrain in the i-th scenario; C^{i}_{river} represents the contribution rate of river backwater effect
224 in the i-th scenario.

225 According to steps (1) to (5), the contribution rates of each waterlogging factors to the

waterlogging degree in the study area can be quantitatively evaluated statistically, and the internal relationships among the waterlogging factors can be revealed.

3.3 Factorial Scenario Design for Sensitivity Analysis

To implement the quantitative framework, a series of counterfactual scenarios were designed to isolate the sensitivity of the flood system to anthropogenic and natural factors.

3.3.1 Rainfall Scenarios

Design rainfall events were generated using the Chicago hyetograph method with a peak coefficient (r) of 0.4. Five return periods (P = 1a, 3a, 5a, 10a, 20a) were selected to represent varying hazard intensities, focusing on short-duration (3 hour) events which are most prevalent in the study area.

3.3.2 Perturbation of Waterlogging Factors

A systematic perturbation approach was applied to the three key factors (Table 1):

1) Drainage Capacity: The maximum flow capacity of pipe sections was increased in steps of 20% (up to 100%) to simulate varying degrees of drainage network retrofitting.

2) Low-lying Terrain: To quantify the intrinsic contribution of topography, a sensitivity-based approach was employed. Although raising ground elevation is challenging in engineering practice (except for new developments), simulating this counterfactual scenario (increasing elevation in steps of 20% of the elevation difference relative to surrounding flat areas, as illustrated in Fig. 4) allows us to isolate the hydrodynamic influence of local depressions.

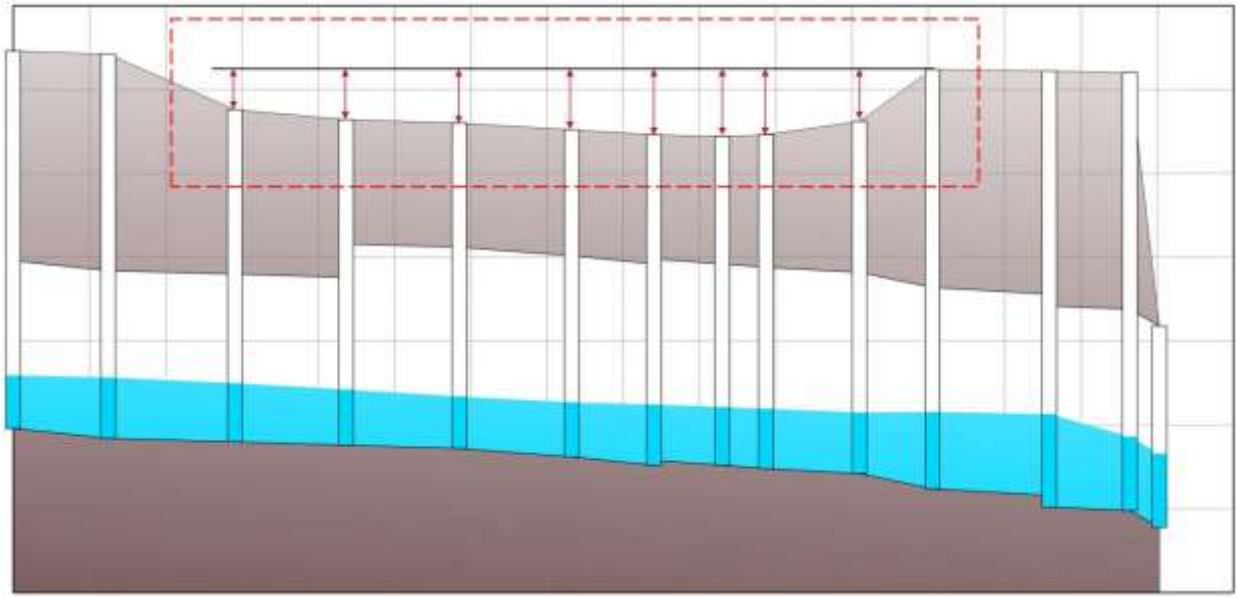


Fig. 4. Schematic diagram of changes in low-lying terrain.

3) River Backwater Effect: The boundary condition at outfalls was adjusted from submerged to free outflow in graduated steps, simulating different river water level control strategies.

Table 1 Simulation scenario design of three waterlogging factors.

Simulation scenario	Maximum flow capacity of pipe section	Inspection chamber rim elevation	River level
Basic Scenario	initial flow	initial ground surface elevation	submerged outflow
Scenario 1	expand by 20%	raise by 20%	just fully submerged
Scenario 2	expand by 40%	raise by 40%	submerge by 60%
Scenario 3	expand by 60%	raise by 60%	submerge by 40%
Scenario 4	expand by 80%	raise by 80%	just not submerged
Scenario 5	expand by 100%	raise by 100%	free outflow

Taking Scenario 1 as an example (Table 2), a factorial combination matrix was constructed to cover all permutations of these factors, enabling the calculation of all main and interaction effects described in Section 3.2.2.

Table 2 Experimental design of waterlogging factors in Scenario 1.

Case	Maximum flow capacity of pipe section	Inspection chamber rim elevation	River level
Case 1	expand by 20%	initial ground surface elevation	submerged outflow
Case 2	initial flow	raise by 20%	submerged outflow
Case 3	initial flow	initial ground surface elevation	just fully submerged
Case 4	expand by 20%	raise by 20%	submerged outflow
Case 5	expand by 20%	initial ground surface elevation	just fully submerged

Case 6	initial flow	raise by 20%	just fully submerged
Case 7	expand by 20%	raise by 20%	just fully submerged

4 Results and Discussion

4.1 Model Performance Evaluation

The calibrated coupled model demonstrated robust performance in reproducing historical inundation events. For the 1D pipe network simulation, the Nash-Sutcliffe Efficiency (NSE) values for shaft water levels across all calibration and validation events exceeded 0.75, with relative peak errors consistently below 6%. For 2D surface flooding, the simulated maximum waterlogging depths at electronic gauge locations showed strong agreement with observed data, with relative errors kept within 20%. These metrics confirm that the coupled model effectively captures the hydrodynamic behavior of the study area under complex boundary conditions. Detailed validation plots and error statistics are provided in the Supplementary Information (Figs. S1-S6). Detailed error statistics and calibration metrics for each rainfall event are provided in Table S1 of the Supplementary Information.

4.2 Disentangling the Non-Linear Interaction Mechanisms

The factorial scenario analysis reveals that urban waterlogging is not a linear summation of individual factors but a result of complex mechanistic interactions (Figs. 5-6).

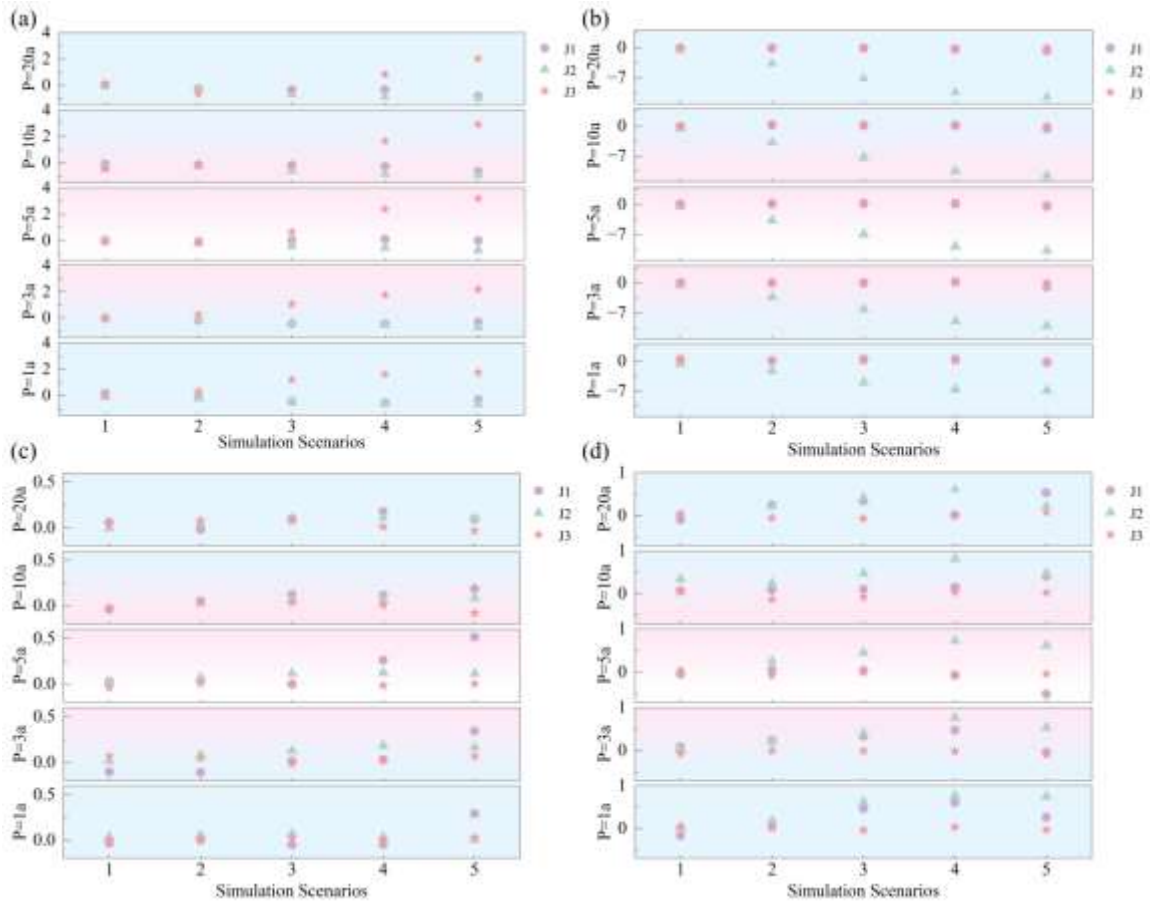


Fig. 5. The interaction effect of three waterlogging factors on the maximum waterlogging depth: **(a)** interaction effects between insufficient drainage capacity and low-lying terrain, **(b)** the interaction between insufficient drainage capacity and river backwater effect**, (c)** the interaction between low-lying terrain and river backwater effect and **(d)** the interactive effects among the three waterlogging factors.

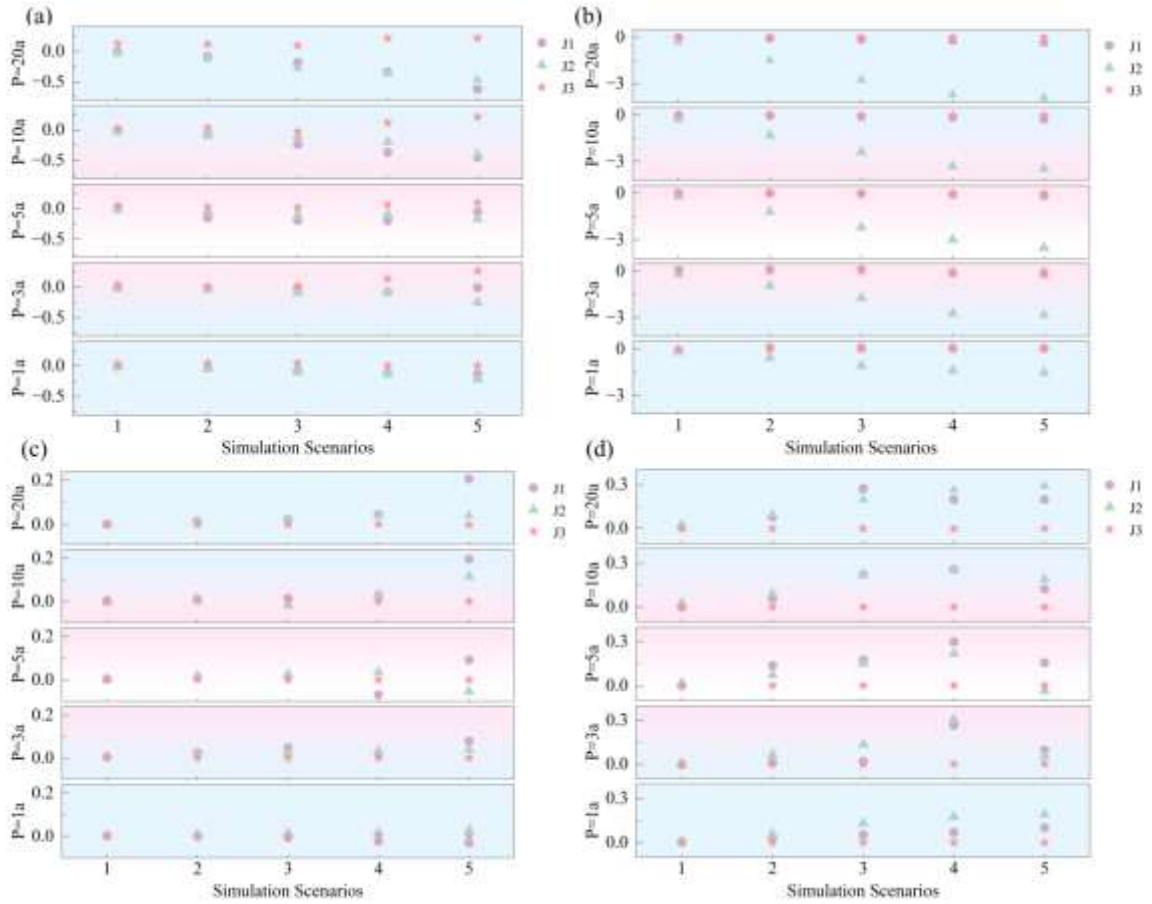


Fig. 6. The interaction effect of three waterlogging factors on the total overflow volume: **(a)** interaction effects between insufficient drainage capacity and low-lying terrain, **(b)** the interaction between insufficient drainage capacity and river backwater effect, **(c)** the interaction between low-lying terrain and river backwater effect and **(d)** the interactive effects among the three waterlogging factors.

(1) Antagonistic Mechanism between Drainage Capacity and Terrain

A consistent antagonistic effect (negative interaction) was observed between insufficient drainage capacity and low-lying terrain across most scenarios. This phenomenon indicates a mechanism of diminishing marginal returns: in distinct local depressions, merely expanding pipe diameters yields progressively smaller benefits if the gravity head is constrained by the terrain itself. The hydraulic bottleneck shifts from the pipe cross-section to the lack of hydraulic gradient, suggesting that conventional grey infrastructure retrofitting (e.g., pipe replacement) faces a theoretical ceiling in low-lying zones.

(2) Synergistic Amplification by River Backwater Effects

In contrast, the interaction between insufficient drainage capacity and the river backwater effect manifests primarily as a synergistic effect, particularly regarding maximum waterlogging depth. This synergy implies a hydraulic lock mechanism: high river stages submerge outfalls, effectively reducing the discharge capacity of the pipe network. When combined with inadequate pipe capacity, this boundary constraint amplifies flood severity beyond the sum of individual impacts. Notably, this synergistic amplification is highly sensitive to the rainfall return period, escalating significantly during extreme events, which underscores the vulnerability of coastal drainage systems to compound flooding.

4.3 Quantitative Attribution of Compound Flood Risks

The contribution rate analysis (Figs. 7-9) further quantifies the spatial heterogeneity of flood drivers, revealing distinct risk typologies among the monitored nodes.

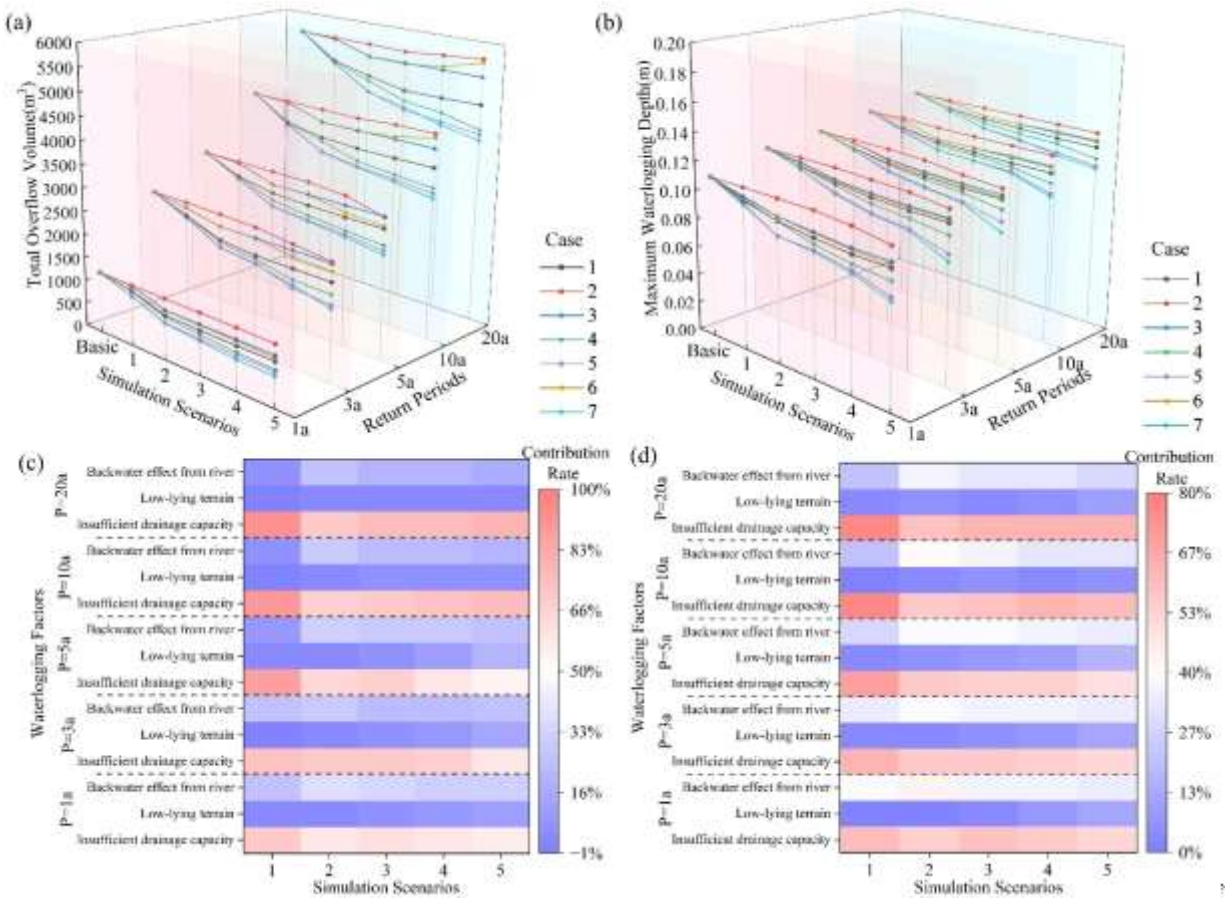


Fig. 7. Simulation results of J1 point waterlogging factors under different return periods: **(a)** total overflow volume, **(b)** maximum waterlogging depth, **(c)** the contribution rates of waterlogging factors to the total overflow volume and **(d)** the contribution rates of waterlogging factors to the maximum waterlogging depth.

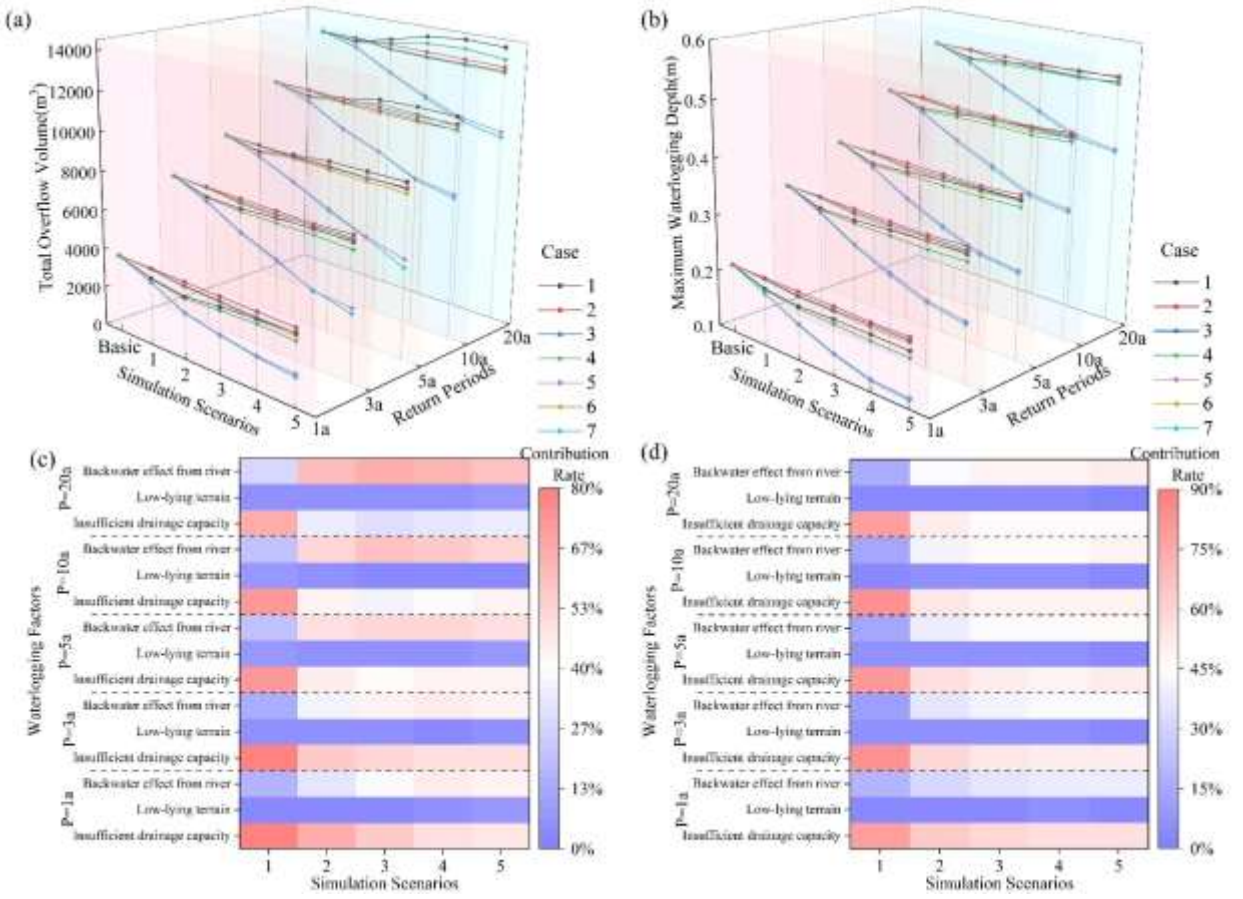


Fig. 8. Simulation results of J2 point waterlogging factors under different return periods: **(a)** total overflow volume, **(b)** maximum waterlogging depth, **(c)** the contribution rates of waterlogging factors to the total overflow volume and **(d)** the contribution rates of waterlogging factors to the maximum waterlogging depth.

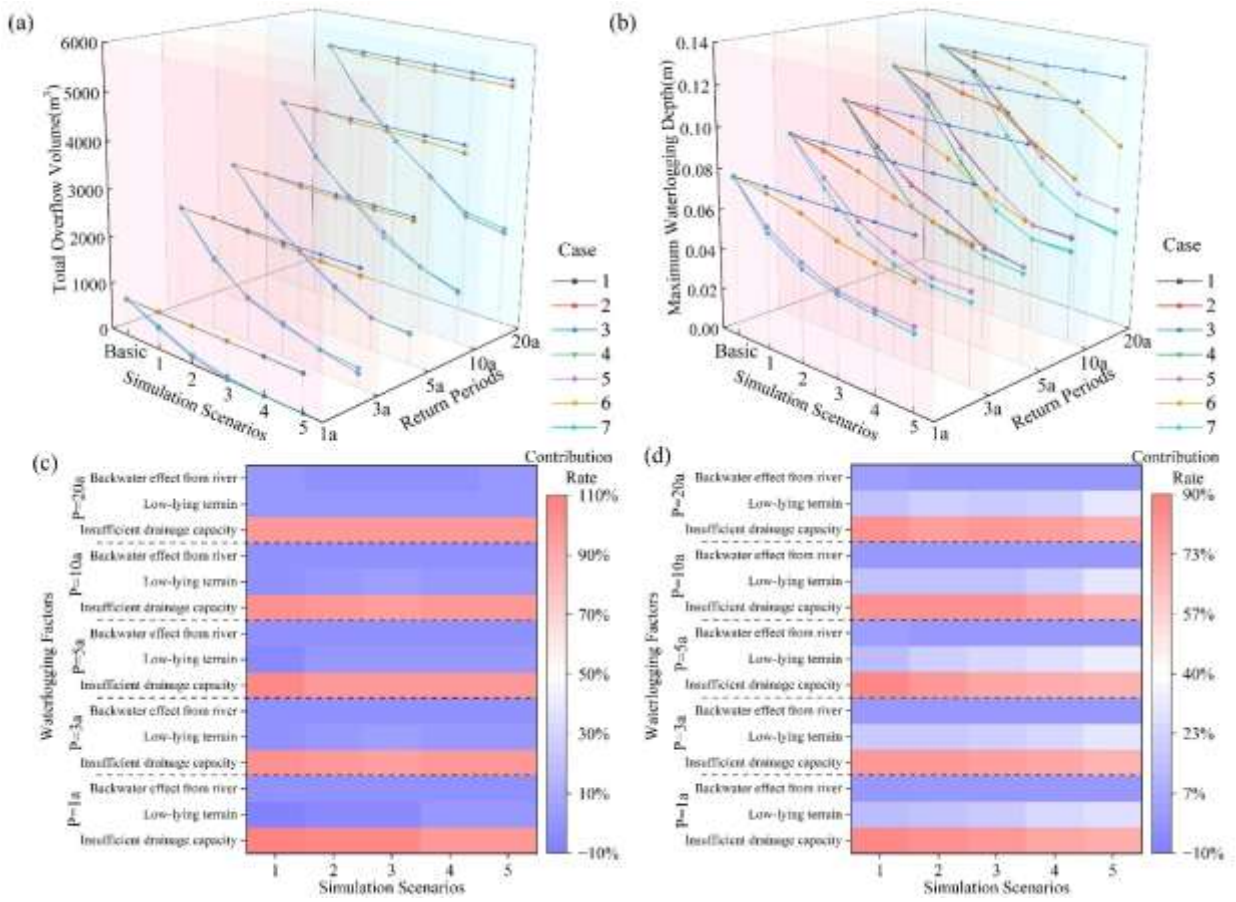


Fig. 9. Simulation results of J3 point waterlogging factors under different return periods: **(a)** total overflow volume, **(b)** maximum waterlogging depth, **(c)** the contribution rates of waterlogging factors to the total overflow volume and **(d)** the contribution rates of waterlogging factors to the maximum waterlogging depth.

(1) Drainage-Dominated Regime

For nodes like J3, insufficient drainage capacity is the overwhelming determinant, contributing nearly 100% to the total overflow volume. The contribution of the river backwater effect remains negligible (near zero) regardless of the return period. This suggests that waterlogging here is strictly a transport capacity issue, independent of downstream boundary conditions.

(2) Boundary-Sensitive Regime

Node J2 exhibits a dynamic shift in risk drivers, characterizing a typical compound flooding regime. Under low return periods (P=1a), drainage capacity is the primary factor. However, as the

return period increases to 20a, the contribution of the river backwater effect surges from 16% to 65% for overflow volume. This dramatic shift indicates that during extreme events, the system transitions from being pipe-constrained to boundary-constrained. The high river levels imposed by intense rainfall create a rigid boundary that nullifies the benefits of upstream pipe expansion.

(3) Topography-Constrained Regime

At Node J1, located in a severe depression, drainage capacity remains the dominant contributor (55% - 92%). However, unlike J2, the relative contribution of the river backwater effect shows a declining trend (decreasing from 37% to 7% for overflow) as the rainfall intensity increases. This counter-intuitive pattern suggests that in deep depressions, the local accumulation rate from surface runoff during extreme storms far outpaces the discharge rate, making the internal drainage limitation more critical than the external river boundary.

4.4 Implications for Resilient Mitigation Strategies

The decoupled mechanisms provide evidence-based insights for optimizing urban flood resilience strategies:

(1) Breaking the hydraulic lock in Coastal Zones: For boundary-sensitive areas (like Node J2), the traditional strategy of solely upgrading pipe networks is ineffective during extreme events due to the dominant backwater effect. Mitigation must prioritize active boundary control, such as installing tidal gates and heavy-duty pumping stations to force drainage against high river stages, rather than passive gravity discharge.

(2) Targeted Retrofitting for Depressions: For topography-constrained zones (like Node J1),

where an antagonistic effect limits pipe efficacy, strategies should focus on surface runoff reduction (e.g., Sponge City interventions) to reduce the inflow load, combined with localized micro-pumps, as gravity-based solutions face diminishing returns.

(3) Cost-Effective Upgrades: For drainage-dominated areas (like Node J3), standard pipe network expansion remains the most cost-effective solution, as the risks are decoupled from downstream river levels.

5 Conclusions

This study addresses the critical challenge of quantifying compound flood risks in high-density coastal cities. By developing a coupled hydrodynamic modeling framework integrated with factorial scenario analysis, the contribution rates and non-linear interaction mechanisms of anthropogenic and natural waterlogging factors in the Shalang area, Zhongshan are successfully disentangled. The main conclusions are as follows:

(1) A Robust Quantitative Framework for Risk Disentanglement

A systematic framework that integrates high-resolution 1D-2D coupling (SWMM and ITF-FLOOD) with a game-theory-based contribution rate analysis is established. This approach overcomes the limitations of traditional linear correlation methods, effectively isolating the synergistic and antagonistic effects hidden within complex compound flooding events. The model demonstrated high reliability (NSE > 0.75), providing a rigorous tool for coastal urban flood management.

(2) Decoupling the Antagonistic Constraint of Terrain

A consistent antagonistic mechanism was identified between insufficient drainage capacity and low-lying terrain. Our findings reveal that in deep topographic depressions, the effectiveness of gravity-based drainage retrofitting (e.g., pipe enlargement) follows a law of diminishing marginal returns. This implies that for topography-constrained zones, relying solely on grey infrastructure expansion is theoretically limited by the lack of hydraulic gradient.

(3) Revealing the Hydraulic Lock Mechanism

The river backwater effect was found to act as a non-linear amplifier of flood risks, exhibiting a strong synergistic effect with drainage limitations. While insufficient pipe capacity is the baseline cause of waterlogging (contributing > 30%), the river boundary condition becomes the dominant constraint during extreme rainfall events (contribution surging to 65% at critical nodes). This hydraulic lock phenomenon confirms that the vulnerability of coastal drainage systems is dynamically modulated by downstream boundary conditions.

(4) Implications for Differentiated Mitigation Strategies

The study advocates for a shift from “one-size-fits-all” pipe upgrades to differentiated, mechanism-based mitigation strategies.

For boundary-sensitive areas subject to the hydraulic lock, active boundary controls (e.g., tidal gates, pumping stations) are essential prerequisites for effective drainage.

For topography-constrained depressions subject to antagonistic effects, source control (Sponge City) and micro-drainage interventions should be prioritized over massive pipe expansion.

For drainage-dominated areas, conventional network optimization remains the most cost-

effective solution.

References

Ding, Q.Y., Xi, X.F. (2024). Cause analysis of urban waterlogging based on SWMM model. Express Water Resources & Hydropower Information. 45(04):31-34+40. http://dx.doi.org/10.15974/j.cnki.slsdkb.2024.04.005

Fan, J.J., Wang, J.L. (2023). An empirical study on the contribution rate of higher education to economic growth in Inner Mongolia. Journal of Inner Mongolia Minzu University. 38(04):301-307. http://dx.doi.org/10.14045/j.cnki.15-1220.2023.04.003

Huber, W.C., Rossman, L.A., Dickinson, R.A. (2005). EPA Storm Water Management Model SWMM 5.0. Washington: Environmental Protection Agency.

Han, F.F., Zhang, X.Y., Yu, J.S., Xu, S.G., Zhou, G.H., Li, S. (2024). Study on spatiotemporal dynamic characteristics of precipitation and causes of waterlogging based on a data-driven framework. The Science of the total environment. 913(02): 169796. http://dx.doi.org/10.1016/J.SCITOTENV.2023.169796

Jin, C.S., Di, S.C., Liu, H.L., Yu, F.Q., Xue, Z.C. (2023). Analysis of the causes of waterlogging and the effectiveness of treatment measures at Jin'an Bridge, a typical waterlogging site in Beijing. Water Resources and Hydropower Engineering. 54(3): 59-71. http://dx.doi.org/10.13928/j.cnki.wrahe.2023.03.005.

Komori, D., Nakaguchi, Kota., Inomata, Ryosuke., Oyatsu, Y., Tachikawa, R., Kazama, S. (2022). Topographical characteristics of frequent urban pluvial flooding areas in Osaka and Nagoya Cities, Japan. Water. 14(18): 2795. http://dx.doi.org/10.3390/W14182795

Lin, J.Y., He, P.T., Yang, L., He, X.Y., Lu, S.Y., Liu, D.Y. (2022). Predicting future urban waterlogging-prone areas by coupling the maximum entropy and FLUS model. Sustainable Cities and Society. (prepublish):103812-.

http://dx.doi.org/10.1016/J.SCS.2022.103812

Luan, G.X., Hou, J.M., Wang, T., Zhou, Q.S., Xu, L.J. Sun, J.H., Wang, C.X. (2024). Method for analyzing urban waterlogging mechanisms based on a 1D-2D water environment dynamic bidirectional coupling model. Journal of environmental management. 360121024-121024. http://dx.doi.org/10.1016/J.JENVMAN.2024.121024

Li, X.C., Zhou, Y., Li, X.H., Zhou, Y., Li, J., Luo, Y., Tang, H.L., Li, S.Q., Lu, Z. Y. (2024). Study on the impact of rural river management on flood disasters under extreme weather conditions: A case study of rural areas in Northern Henan Province. Water Resources and Hydropower Engineering.55(1): 28-39. http://dx.doi.org/10.13928/j.cnki.wrahe.2024.01.003

Pan, Y.H. (2025). Analysis of the construction path of Sponge city from the perspective of urban waterlogging prevention. Ecology And Resources. (01):41-43. http://dx.doi.org/10.20260/j.cnki.styzy.2025.01.014

Singh, H., Nielsen, M., Greatrex, H. (2023). Causes, impacts, and mitigation strategies of urban pluvial floods in India: a systematic review. International Journal of Disaster Risk Reduction. 93, 103751. http://dx.doi.org/10.1016/J.IJDRR.2023.103751

Wang, P., Deng, X.Z., Zhou, H.M., Qi, W. (2018). Responses of urban ecosystem health to precipitation extreme: A case study in Beijing and Tianjin. Journal of Cleaner Production. 177124-133. http://dx.doi.org/10.1016/j.jclepro.2017.12.125

Wu, J.H., Liu, Z.H., Liu, T.X., Liu, W., Luo, H.B. (2023). Assessing urban pluvial waterlogging resilience based on sewer congestion risk and climate change impacts. Journal of Hydrology. 626, 130230 http://dx.doi.org/10.1016/J.JHYDROL.2023.130230

Xu, Q.H., Xiong, L., Zhu, T.L., Xiong, Q.K., Wang, X.Y. (2024). Study on urban waterlogging control modes adapted to cities of different nature condition types in China. Water Resources and Hydropower Engineering. 55(1):11-

27. http://dx.doi.org/10.13928/j.cnki.wrahe.2024.01.002

Zhang, M.L., Xu, M.H., Wang, Z.L., Lai, C.G. (2021). Assessment of the vulnerability of road networks to urban waterlogging based on a coupled hydrodynamic model. Journal of Hydrology. 603, 127105 http://dx.doi.org/10.1016/J.JHYDROL.2021.127105

Zhao, C.H., Wan, J.H., Zhang, Y.X., Zhang, B.W. (2023). Review of the characteristics, causes and governance of urban flood in China. Journal of Catastropholog.38(1): 220-228.http://dx.doi.org/10.3969/j.issn.1000-811X.2023.01.033.

Zheng, J.W., Yin, C.Y., Dai, L., Zhou, F., Zhao, Y.H. (2023). Analysis of spatial and temporal distribution characteristics and driving factors of inundation in karst mountains, Southwest China at multi-scales: Taking Guiyang City as an example. Water Resources and Hydropower Engineering.54(2): 33-46. DOI: http://dx.doi.org/10.13928/j.cnki.wrahe.2023.02.004.

Zhai, M.S. (2023). Simulation and Impact Analysis of Urban Flooding Based on Hydrodynamic Coupling Model—Case study on Lianjiang Middle Road Area in Fuzhou City. Handan. Hebei University of Engineering. http://dx.doi.org/10.27104/d.cnki.ghbjy.2023.001075

Zou, H., He, F., Bai, J.L. (2023). Factors affecting rainfall-induced landslides in Huanggang and its relation with precipitation. Journal of Changjiang River Scientific Research Institute.40(02):124-130.http://dx.doi.org/10.11988/ckyyb.20210841

Statements and Declarations

Funding

This work was supported by the Foundation for Hebei Natural Science Foundation (Grant

No. E2024402142); the Provincial Water Resources Science and Technology Program of Hebei Province (Grant No. HBSL2025-04); and the Xiongan New Area Science and Technology Project (Grant No. 0101017). All authors have read and agreed to the published version of the manuscript.

Competing Interests

The authors declare that they have no known competing financial interests or personal relationships that could have influenced the work reported in this study.

Author Contributions

Yan Long: Conceptualization, Validation, Data Curation, Writing - review & editing, Supervision, Funding acquisition. **Shumin Jiang**: Conceptualization, Methodology, Validation, Writing - Original Draft, Supervision. **Tongxin Yang**: Conceptualization, Methodology, Writing - review & editing, Supervision. **Yikai Hou**: Methodology, Resources, Supervision, Visualization. **Yifan Chen**: Data curation, Visualization, Investigation, Supervision. **Xiaohui Lei**: Conceptualization, Supervision, Project administration, Methodology. **Chenfei Duan**: Writing - review and editing, Supervision, Investigation, Methodology.

Data Availability

The datasets generated during and/or analyzed during the current study are not publicly available due to a data confidentiality agreement, but are available from the corresponding author on reasonable request.

Supplementary Files

This is a list of supplementary files associated with this preprint. Click to download.

- Highlights.docx
- SupplementaryInformation.docx